* Complete Manuscript including All Figs & Tables

Simulation of ceramic furnaces using one-dimensional model of heat transfer – Part I: Model development and validation

Sunil Gokhale [b], M. R. Ravi [a*], P. L. Dhar [a], and S. C. Kaushik [b]

Indian Institute of Technology, New Delhi, India

Abstract

A model for simulating heat transfer in different types of ceramic furnaces has been developed. Typically, the thermal efficiency of conventional batch type ceramic furnaces (kilns) is below 5%. In this study, the firing processes inside a ceramic furnace has been analyzed to predict the gross temperature of the chamber components – wall, ware and gas, throughout the firing cycle using a one-dimensional heat transfer model. The utility of the analysis is in predicting and improving the thermal efficiency of the downdraft as well as updraft ceramic furnaces with minimal computational resources. The data collected during a total of five firings performed on four different kilns has been used to validate this simple model of simulation. The predicted chamber temperature history throughout the firing cycle has been compared with measured temperature. The predicted temperatures compare reasonably well with the measured temperatures.

Keywords: Ceramic, Furnace, Kiln, Simulation, Heat transfer, Firing

[a] Department of Mechanical Engineering, [b] Center for Energy Studies,

* Corresponding Author, Tel.: +91 11 26591059; fax: +91 11 26582053

E-mail address: ravimr@mech.iitd.ac.in (M. R. Ravi).

Postal Address: Department of Mechanical Engineering, Indian Institute of Technology, Hauz Khas, New Delhi – 110016, India

Nomenclature:

Symbols

A	Area (m^2)
C	Specific heat (J/ kg K)
CHAMVEL	Estimated chamber gas velocity
E	Energy
ERTCHT	Error in estimation of chamber temperature
h	Specific enthalpy (J/kg)
htc	Convective heat transfer coefficient (W/ m^2 K)
i	'i' th iteration
i+1	'i+1' th iteration
k	Thermal conductivity (W/ K m)
m	mass (kg)
Q	Heat transfer (J)
t	Time (second)
T	Temperature (K)
TG	Temperature of gas entering the chamber (K)
TIN	Chamber temperature at the beginning of time step (K)
TOUT	Chamber temperature at the end of the time step (K)
TCHT	Actual Chamber (Top) Temperature (K)
TCHT1	Expected thermocouple reading (K)
T1	Pottery surface temperature (K)
T2	Wall inside surface temperature (K)
T3 to N	Wall element (no 3 to N) temperatures (K)
T_{gas}	Chamber temperature used to estimate heat transfer in the kiln (K)
x	Distance (m)

Greek letters:

ρ	Density (kg/ m^3)
σ	Stefan-Boltzman constant

Δ	finite difference – space or time
ε	Emissivity
α	Absorptivity
δ	Differential
Subscripts:	
cv	Control Volume
a	Air
av	Average
amb	Ambient
CB	Ceramic blanket
ch	Chamber
cu	Cumulative
f	Fuel
g	Gas
in	Input to the kiln
out	Exhaust
p	Pottery-ware
w	Brick wall
1 to N	Related to finite elements 1 to N
Superscript	
o	Degree
*	Rate with respect to time

1.0 Introduction:

The pottery industry has been in existence from the pre-historic times, probably from the time man learnt to use fire. Manufacture of ceramics involves firstly control of grain size, moisture and mixing of natural inorganic substances. Then it is formed and heat treated into a sintered state. Although, industrial ceramics are produced using

highly sophisticated furnaces with on-line controls, small potters in developing nations like India still use traditional pottery kilns to produce ceramic ware. Mostly these kilns are wood/ coal fired. In urban/ semi-urban areas in India many kilns are fired with liquefied petroleum gas (LPG) and produce up to 1000 kg of ware in one firing. Typically the small kilns are of about 1 to 4 m^3 in volume. The firing cycles vary from 6 to 50 hour duration.

The firing cycle, which is the temperature vs. time cycle for manufacturing the ceramic material, has typically following stages:

a) Very slow firing (or Smoking): Ambient to 200 ^{0}C @1 deg C/ min, during which residual moisture leaves.
b) Slow firing: 200 to 500 ^{0}C @ 2 deg C/ min, here organic substances are carbonized and combusted (material strength reduces).
c) Medium firing: 500 to 700 ^{0}C @ 3 deg C/ min, here crystalline water of clay minerals leaves, and much energy is needed.
d) Fast firing: 700 ^{0}C to the maximum temperature @ 4 to 5 deg C/min: here the organic substances carbonized earlier are subjected to oxidation beyond 800 ^{0}C and soot removal takes place. Sufficient air is needed for this. If left to cool after reaching 800 ^{0}C, 'biscuit ware' (unglazed earthenware or terracotta) are produced. If the temperature is taken beyond 800 ^{0}C then active sintering takes place, hard & dense ware are produced. Temperature must be raised uniformly. If the body is large, there are temperature gradients, and the wares need to be maintained at maximum temperature for some time (soaking).
e) Cooling: Controlled cooling is done at a predetermined rate.

The ware can be processed in batch mode or continuous mode. In batch processing kilns the mass of the kiln, kiln-furniture, and the ware are all heated and cooled together. While in continuous processing kilns once the process is established, the wares move on trolleys through different temperature zones and get heat treated, but the mass of the kiln at any point is at a constant temperature. The thermal efficiency of a kiln can be defined as the ratio of heat given to the processed ware, to the total heat supplied by the combustion of the fuel. The thermal efficiency of the continuous kilns is higher than the batch type kilns since the latter uses the energy to heat up the kiln body from room temperature to the operating temperatures, in addition to heating the wares.

The typical values of thermal efficiency of kilns are:

1. Traditional Batch Kiln: below 5%
2. Modern batch Kiln: 6 to 13 %
3. Modern Continuous Kiln: up to 25%

It can be seen that batch processing in traditional kilns is not energy efficient. Therefore, it is important to work on improving energy efficiency in the traditional kilns, without increasing their capital cost significantly.

The study of traditional pottery kilns has not received much attention in the literature, and very few publications are found on this subject. Most of the literature available on the subject is from Central Glass & Ceramic Research Institute (CGCRI), Khurja Division [1, 2, and 3]. CGCRI provides a brief history of pottery kilns, and

advises on the choice of wall insulations, assuming a steady inside temperature equal to the maximum firing temperature. Other available publication [4] has analyzed the heat transfer using advanced computational fluid dynamics (CFD) software. This publication mentions a numerical code "LICET-CERAM" that has been developed. It is used to calculate the unsteady combined heat transfer (conduction, convection and radiation) in the furnace using specially extended CFD techniques in the frame of the widely used finite volume method.

From the study of available literature, we can conclude that there is a need to provide a simplified transient simulation of firing cycle to make a gross estimate of the chamber, pottery and wall temperature history, without using advanced and expensive CFD software packages. The present work focuses on the development of a simple one-dimensional model that can be adapted to various classes of furnaces, and can predict the temperatures at various locations in the furnace that help in computing the quantity of energy absorbed by various parts of the kiln and its contents. The methodology takes into account the kiln volume, construction materials, pottery-ware material to be processed, fuel input rate, air supply, and the heat transfer processes of radiation, convection and conduction. The emphasis is on the prediction of chamber, wall and pottery temperature histories, by simulating the heat transfer to various kiln components. The emissivity of wall and pottery-ware as a function of temperature has been accounted for in the computation. The simulated results have been compared with the actual temperatures recorded during experiments done on four different kilns in operation in the field.

2.0 Mathematical Modeling

2.1 One-Dimensional Analogy

The pottery kiln-walls, the pottery ware and the gases in the kiln are all modeled as 1-dimensional entities: they are assumed to be infinitely large in y and z-directions, and their thickness in the x-direction is chosen comparable to their physical thickness: Figure 1 represents the 1-D analogue of the pottery kiln. The entire ware is modeled as two layers of ware of the same thickness on either side of the plane of symmetry, as shown in figure 1. Since in 1-D calculations, dimensions in y and z directions are taken to be unity, and the thickness of the ware plane is matched with actual thickness, the actual volume of the pottery mass is accounted for in the form of weighting parameter in computations of volumetric terms such as energy absorbed. In the same way, the kiln walls are modeled as two parallel walls made up of the same materials as the actual kiln wall. The volume of gas in between the wall and ware is adjusted to be the same as the gas volume of the actual kiln by choosing the spacing between the ware and wall planes accordingly. Likewise, the gap between two layers of ware is chosen to account for the average size of pottery ware. The volume of gas in the kiln is estimated by subtracting the volume of ware and kiln furniture from the total volume with in the kiln walls. Emissivity of the ware and wall materials as function of the temperature has been accounted for. Geometric and flow details have been ignored, and uniform temperature of the gas regions has been assumed. This is often justifiable at higher temperatures since radiation heat transfer equalizes the temperatures inside the kiln.

Computations are performed in only one half of the kiln, assuming symmetry about x = 0. The mass of each substance (ware, gas and kiln wall) is taken from the data for the kiln. Also, the surface areas for convection to atmosphere, as well as convection

and radiation between gases, pottery and kiln wall have been taken from the kiln data. These quantities are the inputs required for the model. Within the solid domain, viz., within the pottery ware and kiln wall, pure conduction is modeled, while between pottery ware and inner walls of the kiln as well as gases, convection-radiation heat transfer is considered.

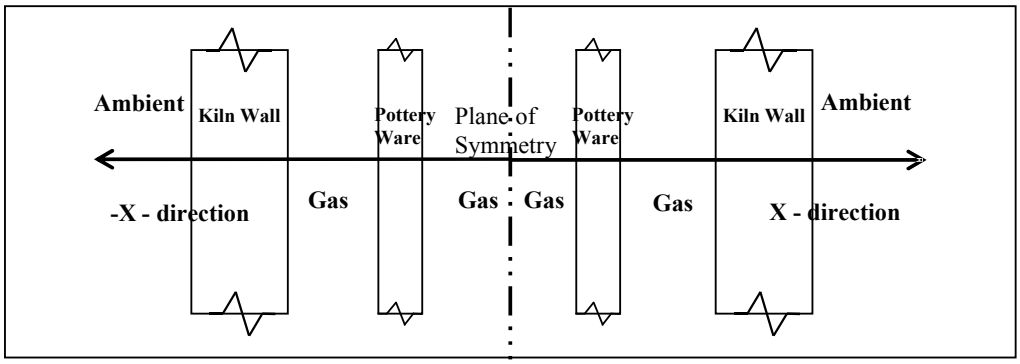

Figure 1: Sketch of 1-D analysis of the pottery kiln.

2.2 Radiation model

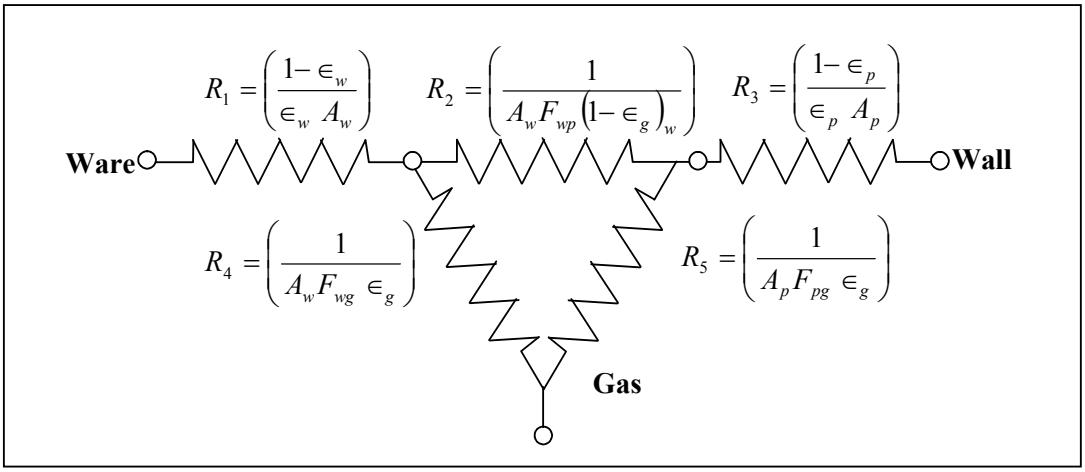

Figure 2: Radiation network between Pottery-ware, Gas and Kiln Wall

The radiation between the wall, the ware and the gases has been modeled using the circuit analogy [5], as illustrated in figure 2. Here, R_1 is the radiative internal resistance

of ware surface and R_3 is the internal radiative resistance of inner surface of the kiln wall. R_2, R_4 and R_5 denote the resistance due to view factors between the three entities.

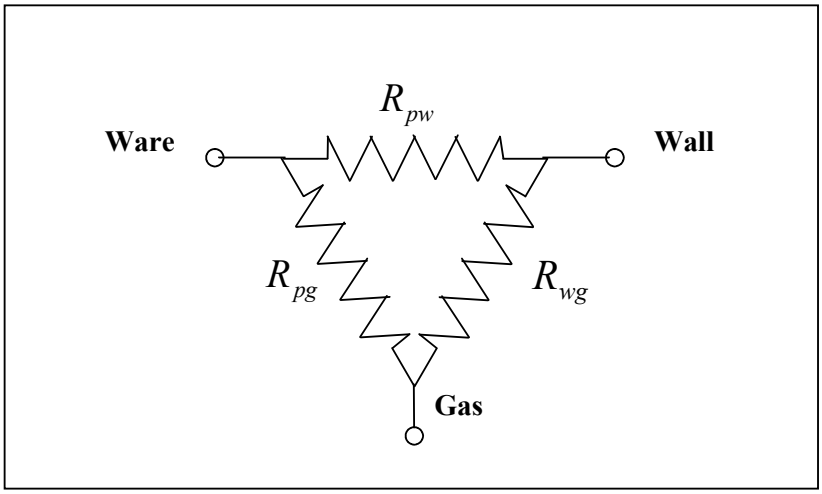

Figure 3: Simplified network between Pottery-ware, Gas and Wall

The circuit in figure 2 is first simplified using Kirchoff's law, into a purely delta form as shown in figure 3, to get: [5] Here,

$$R_A = \left[\frac{R_2.R_4}{R_2 + R_4 + R_5} \right] \qquad R_{1A} = R_1 + R_A$$

$$R_B = \left[\frac{R2.R5}{R2 + R4 + R5} \right] \qquad R_{2A} = R_3 + R_B$$

$$R_C = \left[\frac{R_4.R_5}{R_2 + R_4 + R_5} \right]$$

Where R_1, R_2, R_3, R_4 and R_5 are as described in figure 2. The compound resistances thus obtained are as follows:

$$R_{pg} = \left[\frac{\left(R_{1A}.R_{2A} + R_{1A}.R_C + R_{2A}.R_C\right)}{R_{2A}} \right]$$

$$R_{wg} = \left[\frac{\left(R_{1A}.R_{2A} + R_{1A}.R_C + R_{2A}.R_C \right)}{R_{1A}} \right]$$

$$R_{pw} = \left[\frac{\left(R_{1A}.R_{2A} + R_{1A}.R_C + R_{2A}.R_C \right)}{R_C} \right]$$

Where R_{pg}, R_{wg}, and R_{pw} are the effective resistances between the three entities i.e. the ware, the kiln wall, and the gases, as described in figure 3.

Thus, the radiative heat flow between the three entities, viz, the gas, the ware and the kiln wall can be written as:

Gas to wall: $$Q_{rad,gas-wall} = \sigma \frac{(T_{gas}^4 - T_{wall}^4)}{R_{wg}} \quad (1)$$

Gas to ware: $$Q_{rad,gas-ware} = \sigma \frac{(T_{gas}^4 - T_{ware}^4)}{R_{pg}} \quad (2)$$

Wall to ware: $$Q_{rad,wall-ware} = FWP \cdot \sigma \frac{(T_{wall}^4 - T_{ware}^4)}{R_{pw}} \quad (3)$$

FWP is the view factor between wall and ware, which is taken to be 0.5 since only one side (half) of the ware surface sees the wall.

2.3 Mass & Energy balance

The domain is in three parts namely gas, ware and wall. The energy equation for the ware and the wall is simply the transient one-dimensional heat conduction equation:

$$\frac{\partial T}{\partial t} = \alpha \frac{\partial^2 T}{\partial x^2} \quad (4)$$

For the gaseous part of the domain, the temperature is computed using the mass and energy balance equations written for the gases in the kiln control volume. The radiative and convective heat transfer between the gas and the kiln walls or the wares appear

both as boundary conditions for the solid domains and as the heat transfer terms for the gas domain.

Gas Domain: The control volume shown in dotted line in figure 4 is the gas domain i.e. the volume in the kiln, available for the gas to occupy. The rate of change of mass of gas contained in the chamber volume is given by the difference between the rate of mass inflow of fuel and air and the rate of outflow of mass of flue gas. Here, a change of mass of gases inside the kiln takes place due to change in the density of the gases in the kiln owing to temperature change.

$$\frac{d}{dt}(m_{CV}) = \dot{m}_{in} - \dot{m}_{out}$$

i.e, $$V_{CV}\frac{d}{dt}(\rho_{CV}) = \dot{m}_{fuel} + \dot{m}_{air} - \dot{m}_{flue}$$

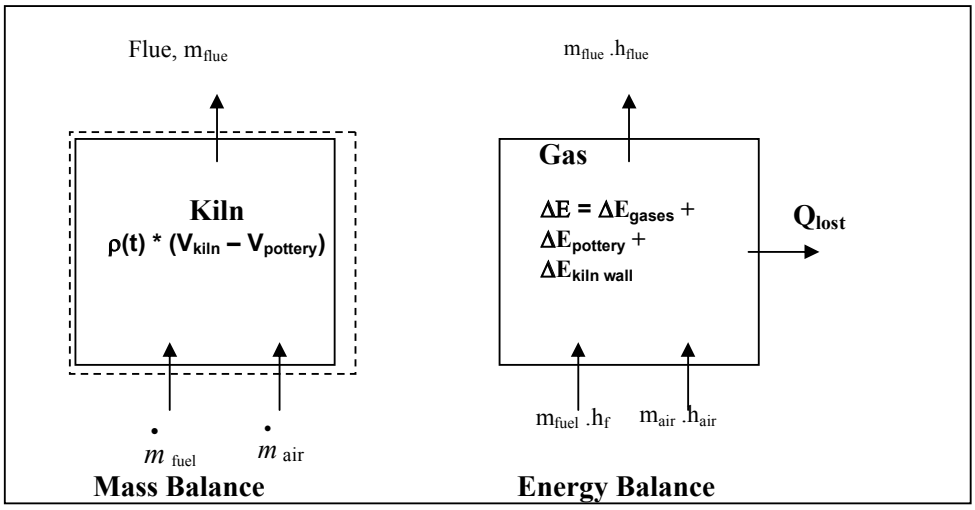

Figure 4: Mass & Energy Balance for the kiln.

The fuel flow rate as a function of time is obtained from the data of actual firing of the kiln. The gas temperature at any instant of time is computed by the energy balance over all three kiln domains. Thus the difference between the total enthalpy of mass (air +

fuel) entering the kiln, and the total enthalpy of the flue gas exiting contributes to the increase in temperature of chamber gas, ware, wall and heat lost to the ambient.

The enthalpy of gas entering the chamber is computed using energy balance as given below:

$$\frac{dE_{cv}}{dt} = \sum \dot{m}_{in} . h_{in} - \dot{m}_{out} . h_{out} - \dot{Q}_{lost}$$

The rate of mass leaving the chamber is computed as follows:

$$\dot{m}_{out} = \dot{m}_{in} - \frac{(\Delta\rho)_{cv}}{\Delta t} V_{cv}$$

The enthalpy of the gas leaving the chamber is computed as follows:

$$h_{out} = C_p (\frac{T_{t+\Delta t} + T_t}{2})$$

$$\frac{(m_{cv} . u_{cv})_{t+\Delta t} - (m_{cv} . u_{cv})_t}{\Delta t} = (\dot{m}_{fuel} . h_{fuel} + \dot{m}_{air} . h_{air}) - \dot{m}_{out} . h_{out} - \dot{Q}_{ware} - \dot{Q}_{wall} \qquad (5)$$

Ware and Wall Domains:

The ware and wall are organized into finite control volumes of equal thickness. In the cases studied the ware thickness was about 6.3mm and therefore ware has been taken as single control volume, while the wall is divided into control volumes of 6.3mm thickness (for kiln#1 & kiln#2) and or 12.6mm thickness (for kiln#3 & kiln#4). There are N control volumes in all, of which the first is the ware and the control volumes numbered 2 to N are in the kiln wall. Values of N in different cases are reported with the response results.

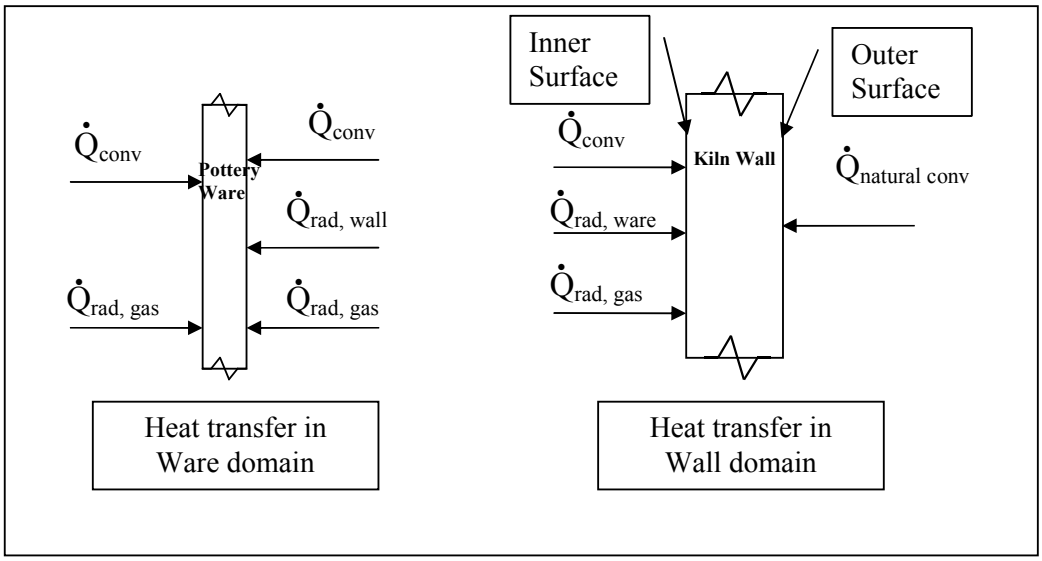

Figure 5: Heat transfer in ware and wall domains

As shown in figure 5, the wares exchange heat with the gas by convection and radiation from both sides. The exchange of heat with the wall is only from one side. A_p and m_p are the total surface area and total mass of all the ware loaded in the kiln, respectively. The temperature in the pottery-ware control volume, T_j (where j=1) is determined from its energy balance:

$$m_p * C_p * \frac{\partial T_j}{\partial t} = A_p * \left(\dot{Q}_{rad,gas-ware} + \dot{Q}_{conv} + \dot{Q}_{rad,wall-ware} \right) \qquad (6)$$

$\dot{Q}_{rad,gas-ware}$ and $\dot{Q}_{rad,wall-ware}$ are given by equation (2), and (3) respectively.

$$\dot{Q}_{conv} = h_{ch}.\left(T_{gas} - T_j\right)$$

Wall Domain:

All the walls including the base and the roof constitute the wall domain that exchanges energy with the gas, ware and ambient. The wall is divided into elements of 6.3mm thickness. As shown in figure 5, the wall exchanges heat with gas by convection and

radiation from one side. The exchange of radiation with the ware is from one side. Natural convection has been considered for the heat loss from the outer surface of kiln wall. Within the wall the heat transfer is by conduction only. From the energy balance for the wall we get:

Wall element of inner surface of kiln, temperature T_j where j=2

$$kA_{wall}[\frac{\partial T_j}{\partial x}]_{x=x_w} = \dot{Q}_{conv,wall} - \dot{Q}_{rad,wall-ware} + \dot{Q}_{rad,gas-wall} \tag{7}$$

where $x=x_w$ is at the inner surface of the kiln wall.

$$\dot{Q}_{conv,wall} = h_{ch}.(T_{gas} - T_j) + k_w \frac{\partial^2 T_j}{\partial x^2}$$

$\dot{Q}_{rad,wall-ware}$ and $\dot{Q}_{rad,gas-wall}$ as given in equation (3) and (1) respectively.

The interior control volumes of wall body exchange heat by conduction alone, and are represented by the finite difference form of equation (4): *T_j where j=3 to (N-1)*

$$\rho.C_v(\frac{T_j^{i+1} - T_j^i}{\Delta t}) = k(\frac{T_{j+1}^{i+1} - 2.T_j^{i+1} + T_{j-1}^{i+1}}{\Delta x^2}) \tag{8}$$

The control volume on the outer surface of the wall exchanges heat with the ambient by natural convection. Outermost Wall temperature, say *T_j where j=N*:

$$-kA[\frac{\partial T_j}{\partial x}]_{x=X} = \dot{Q}_{natconv} \tag{9}$$

$$\dot{Q}_{natconv} = h_{amb}.(T_j - T_\infty)$$

h_{amb} = 3.5 W/m.K is assumed.

2.4 Solution of Discrete Equations:

Equations 6 to 9 are discretized using Simple Implicit Scheme, to solve for the ware and wall temperatures. Here temperature of a control volume in time step (i+1) is a function of temperature of time step (i), the temperature of neighboring contol volumes in the time step (i+1) and the source terms. The equations need to be solved simultaneously using tri-diagonal matrix algorithm (TDMA).

2.5 Physical properties

Emissivity of gases: The CO_2 and H_2O volume fractions determine the emissivity of the kiln gases. From the fuel flow rate and the gas analysis available as input, we calculate the mole fraction of CO_2 and H_2O and emissivity of the gas is estimated using standard graphs [6].

Specific heat of gases: The specific heat of CO_2, N_2, O_2 and water vapor as a function of temperature are available in literature [6]. These are integrated with respect to temperature and used to back calculate the temperature of the gas mixture from computed enthalpy.

Density of gas: The ideal gas model is used to compute the density of the gas with respect to temperature of the gas for each time step.

Emissivity of wall and ware surface: Data on surface emissivity of these materials as a function of temperature have been used from the literature [6].

2.6 The input Parameters

The following input parameters are required for the model:

- Fuel composition and rate of consumption throughout the firing cycle

- Kiln geometry & material properties including the ware to be processed
- Ambient temperature
- Total firing time
- Chamber CO_2 composition as a function of time
- Standard formulae to estimate complete gas composition (O_2, CO_2, N_2, H_2O) on the basis of fuel composition & the CO_2 percentage measured during the experiment.
- Estimation of natural convection heat transfer coefficient for the ambient.

2.7 Solution Methodology

1. A small time step Δt seconds is chosen. The $(i)^{th}$ time step is the initial conditions of the chamber, starting from i = 1 i.e. the ambient conditions. We perform calculations for the $(i+1)^{th}$ time step. (At time = 0 or at the start of the process, i = 1)

2. The recorded rate of fuel input and excess air (calculated from the measured CO_2 composition) are used to calculate the enthalpy of the gases entering the chamber (h_g). The initial mass, temperature and enthalpy of the chamber gas are known. The mass of fuel, its calorific value, and mass of air entering in the current time step are used in equation (5) to calculate resultant enthalpy of the chamber gas. Expressions of specific heat as a function of temperature for various gases of the chamber are used to back-calculate the chamber gas temperature. This temperature (T_{IN}) is utilized to estimate the heat transfer between the gas and the ware and the wall.

3. The kiln components i.e. the wall and pottery are divided into finite control volumes of suitable thickness Δx. All the elements are analyzed for heat transfer through Simple Implicit scheme and solved using the tri-diagonal matrix algorithm.

4. Since at the first instance the heat transfer was calculated using T_{IN} as gas temperature, the process is repeated by using T_{CH} as gas temperature. The difference in the T_{CH} estimate for the two consecutive iterations (within the time step ΔT) is calculated and the iterations are repeated, until the T_{CH} converges within a stipulated value.

5. At the end of the time step the resultant chamber gas enthalpy and temperature are calculated, and the temperatures of the wall and the pottery components are calculated.

6. The net and cumulative heat flow to various components of the kiln is calculated.

7. The process is repeated by following step 3 to 6, for the next time step, till all steps for the complete firing time are complete.

8. The output is:

a. The temperature history of all elements of wall and pottery, and

b. Step-wise and cumulative heat transfer to various kiln components.

9. The predicted chamber temperature T_{CH} is to be compared to the Chamber Top Temperature T_{CHT} recorded during the experiment. Since the thermocouple used to

record the chamber top temperature does not have any radiation shield, a radiation compensation calculation is used to adjust T_{CH}. This gives us the simulated thermocouple reading T_{CHT1}, which is then compared with T_{CHT}.

a) Heat exchanged by thermocouple with chamber gas by convection:

$$A_3 = h_{ch} * \left(T_{CH} - T_{CHT1}\right)$$

b) Heat exchanged by thermocouple with chamber gas by radiation:

$$B_3 = \varepsilon_w * \sigma * \left(\varepsilon_g * {T_{CH}}^4 - \alpha_g * {T_{CHT1}}^4\right)$$

c) Heat exchanged by thermocouple with chamber wall by radiation:

$$C_3 = \varepsilon_w * \sigma * \left({T_2}^4 - {T_{CHT1}}^4\right)$$

The following energy balance equation is solved for T_{CHT1}, which is the expected thermocouple reading when the gross chamber temperature is $T_{CH}(i+1)$.

$$A_3 + B_3 + C_3 = 0$$

T_{CHT1} is then compared with the recorded chamber top temperature T_{CHT}.

3.0 Experimental set-up for validation on Kiln#1

To validate the predictions of the model described in the previous sections on different types of kilns, experiments were conducted on three different kilns, referred to as kiln#1, kiln#2 and kiln#3 in this paper. The kiln#1 is LPG fired, and down draft type. The hot gases from the burners enter the chamber from below and go over the ware,

then take an 180° turn and come down to the flue gas exit. The schematic of kiln#1 is given in figure 6.

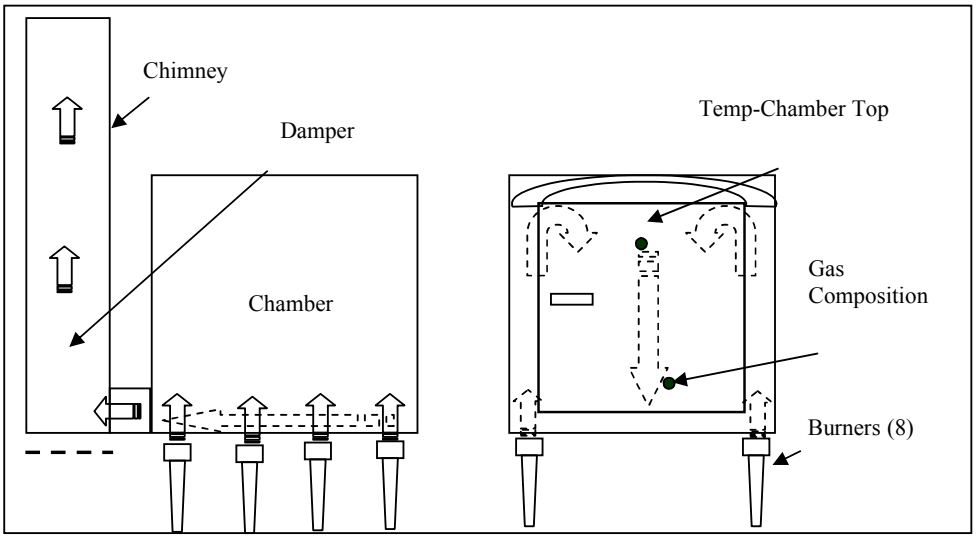

Figure 6: Schematic of a downdraft kiln#1

The details of the kiln construction, payload and firing schedule are described in appendix-I. The instruments used for measurements are described in table-1. The temperature and CO_2 data are used to estimate the furnace firing performance. The furnace is controlled using the damper in the chimney to regulate the flow of gases.

Table 1: Kiln#1 experiment: Instruments used for measurements

S. no.	Instrument	Type	Accuracy
1	Thermocouple with digital indicator	R-Type	+/- 2 ^{o}C
2	Gas Analyzer	Non-Dispersive Infrared (NDIR)	+/- 3% CO_2
3	Weighing Scale	Mechanical	+/- 0.5 kg

Depending upon the actual rate of temperature rise vis-à-vis the firing cycle, fuel flow control valve and the damper are operated to run the firing cycle in the furnace. If the excess air is on the higher side and the temperature does not rise as intended, then damper is pushed further into the gas path to reduce the excess air. If the excess air is within limits then to achieve a firing schedule fuel valve is opened more. If the temperature rise is faster than planned then fuel flow is reduced.

3.1 Validation of results:

The model for 1-D simulation discussed in Section 2 has been coded in a FORTRAN program. This program was run to simulate the experiments described above. The measured chamber top temperature and simulated chamber temperatures were compared. The comparison of the measured and simulated temperatures is given in figure 7. The number of grid points N in the wall of the model of kiln#1 was 37. Simulated temperature is a measure of average chamber temperature and moves on both sides of the recorded chamber top temperature. The root mean square (rms) deviation is 13.15%, which is reasonable. The deviation of predictions from measurements can be attributed to the following reasons:

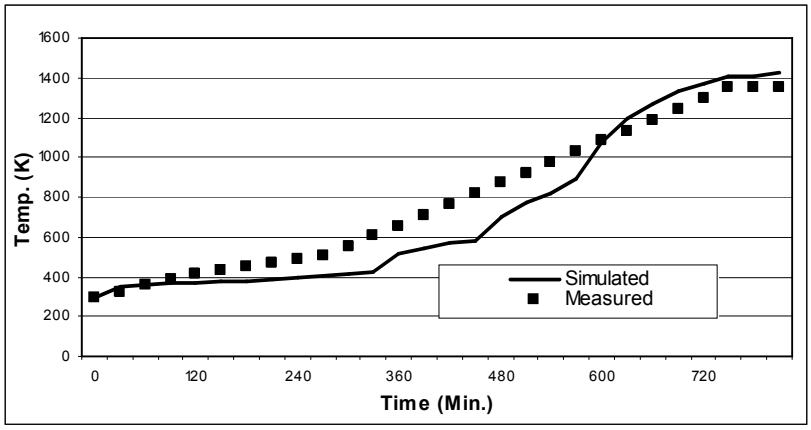

Figure 7: Comparison of predicted & measured chamber temperatures, Kiln#1

- The model estimates gross chamber temperatures, and ignores the effect of gas flow, and the relatively cold and hot regions in the chamber. Therefore, the gross estimate shall be different from the temperature measured at a specific point in the chamber. Hence the measured and simulated temperatures are different.
- Fuel flow measurement during the experiment: The weighing scale had an accuracy of +/- 0.5 kg and the measurements were taken every 30 minutes.
- The thermocouple used for chamber top temperature had an accuracy of +/- 2°C, and were recorded every 15 minutes.
- The chamber gas composition was measured at a frequency of about 30 minutes, while the temperature was measured every 15 minutes. The variations occurring in between have not been accounted for.

Notwithstanding the deviations, the predictions are agreeing fairly in trend and values with measurements, and hence can be used with confidence for simulating modified firing conditions to optimize the thermal efficiency of the system.

3.2 Energy distribution in the kiln#1:

The pie-chart given in figure 8 indicates the predicted distribution of energy to various kiln components. The efficiency of the furnace is low at 3.42%. Heat transfer to inner wall is high at 38%, since the inner wall is made of insulating bricks of high thermal mass. The heat to outer wall is low at 2.5% because of its material of construction - ceramic blanket. Enormous amount of heat (53%) is being lost to the atmosphere with the exhaust gases.

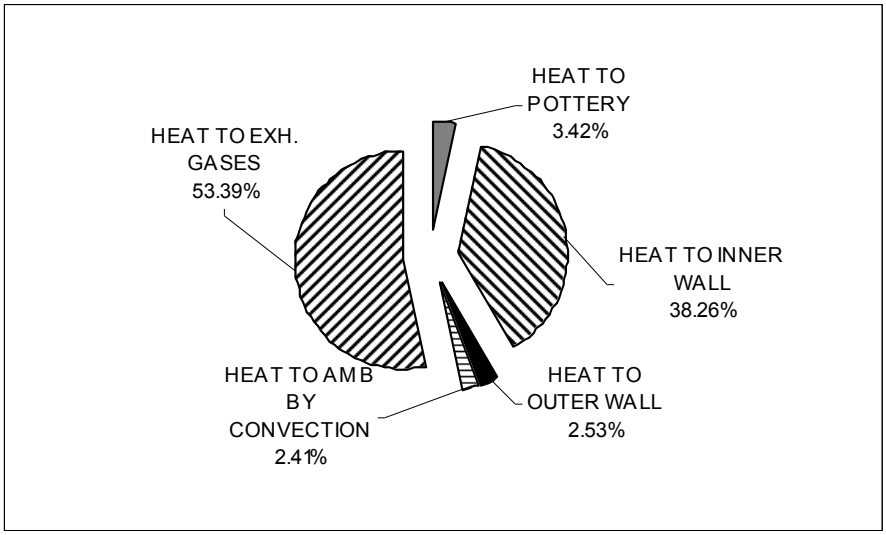

Figure 8: Distribution of heat to kiln components in kiln#1.

3.3 Inferences from the experiment and simulation:

From the above we can infer that we need to reduce the thermal mass of the inner wall, which is accounting for 38% heat. The exhaust gas is taking away 53% of the heat. This needs to be minimized by reducing the gas flow to the bare minimum to achieve complete combustion of the fuel. But since the kiln#1 is a privately owned studio pottery ware kiln, we could not make any modifications into it. Keeping this in mind,

kiln #2, a laboratory scale LPG fired kiln with reduced thermal mass, was designed and fabricated.

4.0 Experimental set-up for validation on Kiln#2

The kiln#2 is also LPG fired, and down draft type. The hot gases from one burner enter the kiln from the bottom, go over the ware then take a 180 ^{o} turn and come down to the flue gas exit. The natural draft of a chimney is used to expel the flue gases. The schematic of the down draft kiln is given in figure 9.

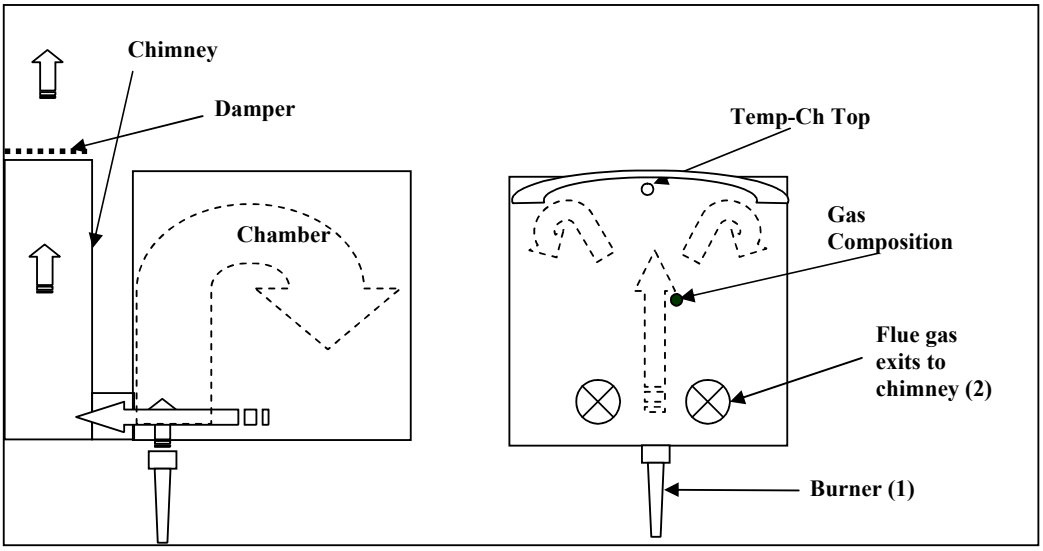

Figure 9: Schematic of a downdraft kiln#2

Table 2: Kiln#2 experiments: Instruments used for measurements

S. no.	Instrument	Type	Accuracy
1	Thermocouple	R-Type	+/- 2°C
2	Gas Analyzer	Non-Dispersive Infrared (NDIR)	+/- 3% CO_2
3	Gas Flow meter	Variable area, float type	+/- 2 %

The details of construction, firing cycle and payload for this kiln are given in appendix II. The instruments used for measurements are listed in table-2. Two experiments were conducted on this kiln:

A) Kiln#2, Experiment#1 Firing cycle:

The firing cycle followed was:

1. Ambient (30 ^{0}C) to 150 ^{0}C @ ~0.8 ^{0}C/min.

2. 150 ^{0}C to 750 ^{0}C @ 2 to 3 ^{0}C/min.

The firing cycle (heating) lasted for 350 minutes.

B) Kiln#2, Experiment#2 Firing cycle:

The firing cycle followed was:

1. Ambient (30 ^{0}C) to 200 ^{0}C @ ~1.5 ^{0}C/min.

2. 200 ^{0}C to 700 ^{0}C @ 2 to 3 ^{0}C/min.

3. Soaking at 700 ^{0}C for 30 min.

The firing cycle (heating) lasted for 260 minutes.

4.1 Validation of results:

The model for 1-D simulation was run to simulate the experiments described above. The measured chamber top temperature and simulated chamber temperatures were compared. The comparison of the measured and simulated temperatures is given in figures 10 and 11 for kiln#2, experiment#1 and 2 respectively. The number of grid points N in the wall region in these simulations is 55.

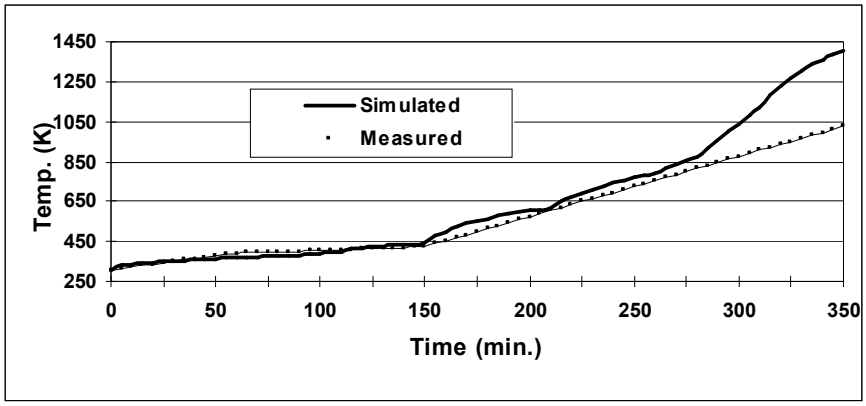

Figure 10: Comparison of predicted & measured chamber temperatures Kiln#2, Exp#1

The predicted temperature is a measure of average chamber temperature and moves on both sides of the measured Chamber Top temperature. The rms deviation is 13.85% and 6.92 % respectively in the two experimental cases. Given the simplicity of the model, the overall performance of the model is reasonably good and it can be used to predict modified firing conditions to optimize the thermal efficiency of the system.

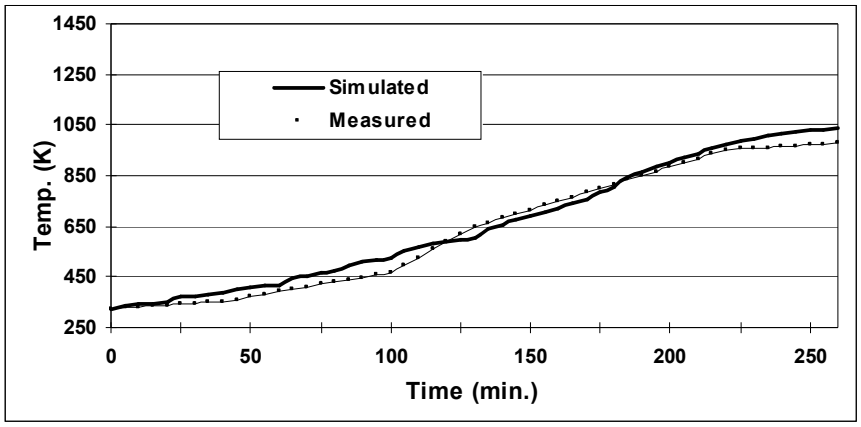

Figure 11: Comparison of predicted & measured chamber temperatures Kiln#2, Exp#2

4.2 Energy distribution in the kiln#2:

The pie-charts given in figures 12 and 13 indicate the distribution of heat energy to various kiln components during experiments 1 and 2, respectively. The changes observed vis-à-vis the previous experiment on kiln#1 are:

1. The efficiencies for the two experiments are on kiln#2 are 15.75% and 10% respectively. The reason of difference is the higher air flow rate in Exp#2. The efficiency of kiln#1 was 3.42% only. In other words, total fuel consumption in kiln #1 was about 30 times that is needed to fire the payload, while in kiln #2 it was between 7 and 10 times, which is substantially lower. This figure also depends heavily on the maximum temperature of firing. In kiln #1, the peak temperature was 1075°C in comparison with kiln #2 where the peak temperature was only 700-750°C. The efficiency would have been lower for kiln #2 for a higher firing temperature.
2. Heat to inner wall is between 10 to 13% which is lower than 38% in kiln#1, because the inner wall is made of ceramic modules of very low thermal mass. The heat to outer wall is negligible, because of the inner wall, which does not allow any heat to flow out through the walls. Again, comparing the energy absorbed by the wall as a function of heat to payload, kiln #1 shows a 10-fold energy going to the walls, while kiln #2 shows almost the same order of magnitude of energy going to the payload and inner walls of the kiln. Even with peak temperature going upto 1075°C, kiln #2 would not have absorbed an order of magnitude higher quantum of energy.

3. But still an enormous fraction of heat (70 to 80%) is still being lost to the atmosphere with the exhaust gases. But even this is only 5-8 times the heat absorbed by the payload in kiln #2, as against a factor of more than 20 in kiln #1.

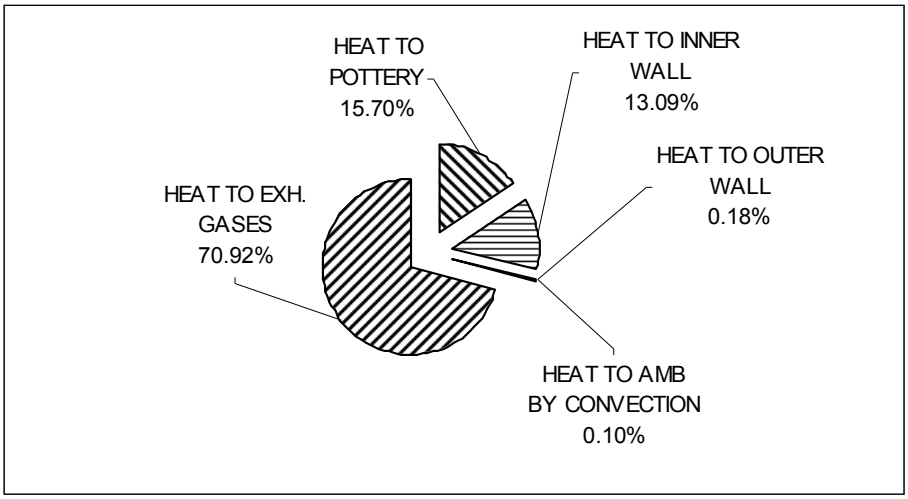

Figure 12: Distribution of heat to kiln components in Kiln#2, Exp#1

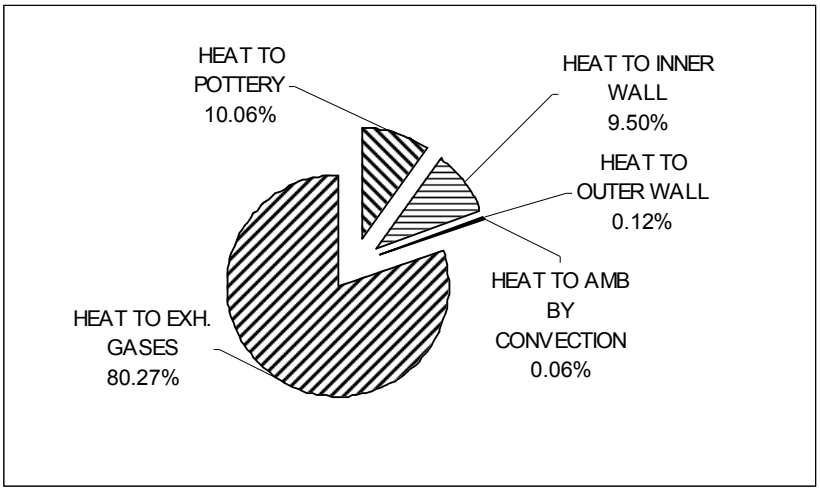

Figure 13: Distribution of heat to kiln components in Kiln#2, Exp# 2.

4.3 Inferences from the experiments and simulation:

1. By reducing the thermal mass of inner wall the heat absorbed by the - inner and outer wall has reduced considerably.
2. The thermal efficiency has improved from 3-4%, to 10-15%.

3. While the heat to the wall has reduced and efficiency has improved, the share of heat flowing out with the flue gas has increased from 53% in Kiln#1 to 70-80% in kiln#2. Therefore, we need to develop a strategy to reduce the flow rate of gases to the bare minimum i.e. just sufficient to effect complete combustion. This shall reduce the quantity of heat carried away by the exhaust gases.

5.0 Experimental set-up for validation on Kiln#3

To validate the model on an updraft kiln an experiment was conducted on kiln#3, an updraft type, wood-fired kiln traditionally used by village potters. The hot gases from the fire box, which is fed from four fire mouths with wood, enter the kiln from the bottom, go over the ware and come out from the flue gas exits at the top. The natural draft developed within the kiln is used to expel the flue gases. The schematic of the updraft kiln is given in figure 14. The details of construction, firing cycle and measurements made in the kiln are listed in appendix-III. The instruments used for measurements are listed in table-3.

Table 3: Kiln#3 experiment: Instruments used for measurements

S. no.	Instrument	Type	Accuracy
1	Thermocouple with digital indicator	R-Type	+/- 2 ^{o}C
2	Weighing Scale	Mechanical	+/- 1 kg

The flue gases come out of the openings at the top of the kiln and therefore we have to use flame temperature to estimate the excess air supplied. The flow of gases in the furnace is not controlled, since it does not have any fixed gas outlet where a damper

can be fixed. Depending upon the actual rate of temperature rise vis-à-vis the firing cycle, fuel input is controlled by skillful artisans to run the firing cycle. If the temperature rise is faster than planned then fuel flow is reduced.

5.1 Validation of results:

Comparison of the measured and simulated ware temperatures is given in figure 15. Simulated temperature is a measure of average ware temperature and moves on both sides of the recorded Chamber Top temperature. The root mean square (rms) deviation is 4.83 %, which indicates a good agreement. The number of grid points N in the wall region for the simulation of kiln#3 is 41.

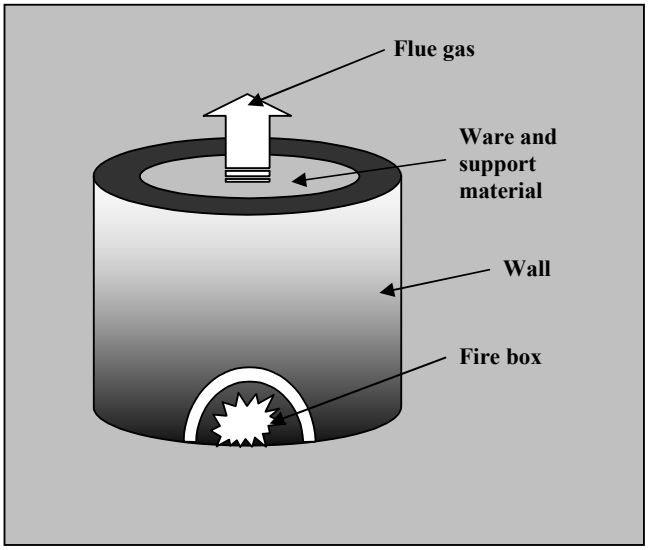

Figure 14: Schematic of a updraft kiln#3

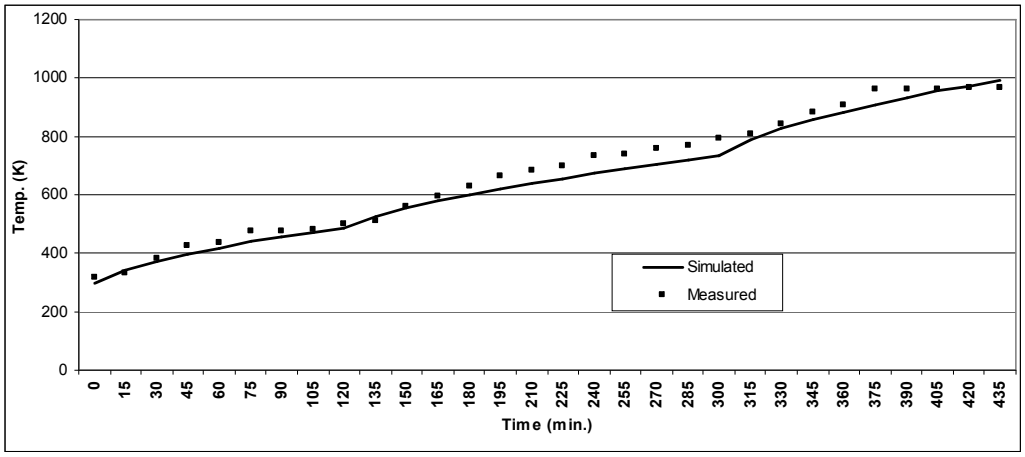

Figure 15: Comparison of predicted & measured ware temperatures, Kiln#3

5.2 Energy distribution in the kiln#3:

The pie-chart given in figure 16 indicates the predicted distribution of energy to various kiln components. The efficiency of the furnace is 8.89%. Heat transfer to the wall is very high at 62.76%. A large amount of energy (28.32%) is being lost to the atmosphere with the exhaust gases.

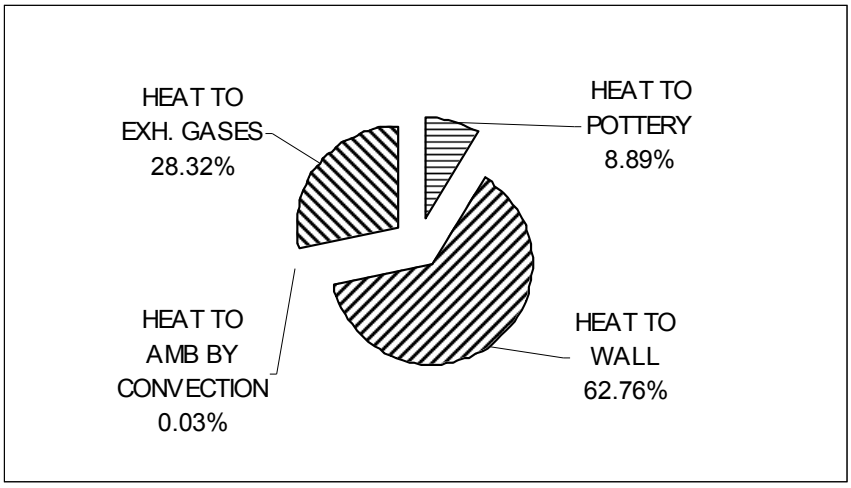

Figure 16: Distribution of heat to kiln components in kiln#3.

5.3 Inferences from the experiment and simulation:

From the above we can infer that we need to reduce the thermal mass of the inner wall, which is accounting for 62.76% heat. The exhaust gas is taking away 28.32% of the heat. This needs to be minimized by reducing the gas flow to the bare minimum to achieve complete combustion of the fuel.

6.0 Experimental set-up for validation on Kiln#4

To validate the model on another updraft kiln an experiment was conducted on kiln#4. The kiln#4 is also an updraft type, wood-fired kiln as shown in figure 14. It differs from kiln#3 in that it uses rat-trap bond construction (figure 17) that allows for air gap within the brick wall, thus making the structure lighter, and thermally more insulating. The wall is in 2 parts, the inner wall with the rat-trap bond construction and the outer wall of red brick construction.

For the inner wall equivalent wall thermal conductivity has been calculated taking into account the innermost 76 mm brick, middle layer of 76 mm of brick and air (66.66% air gap), and the outermost 76 mm brick layer. For outer wall is 152 mm of brick.

The fuel flow rate, flame temperature and ware temperatures were recorded as indicated in appendix IV. The same instrumentation as listed in table 3 were used in this experiment as well. The method of control of temperature rise rate is the same as described in the case of kiln #3.

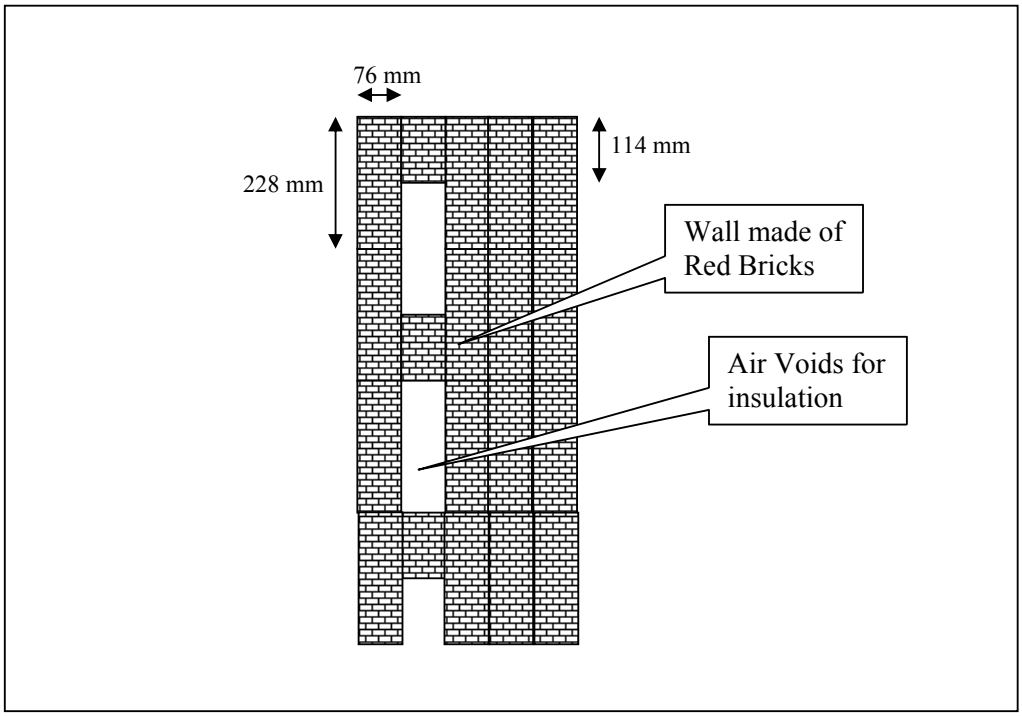

Figure 17: Rat-trap bond construction of the wall in kiln# 4

6.1 Validation of results:

Comparison of the measured and simulated ware temperatures is given in figure 18.

The N value for simulation of kiln#4 is 31.

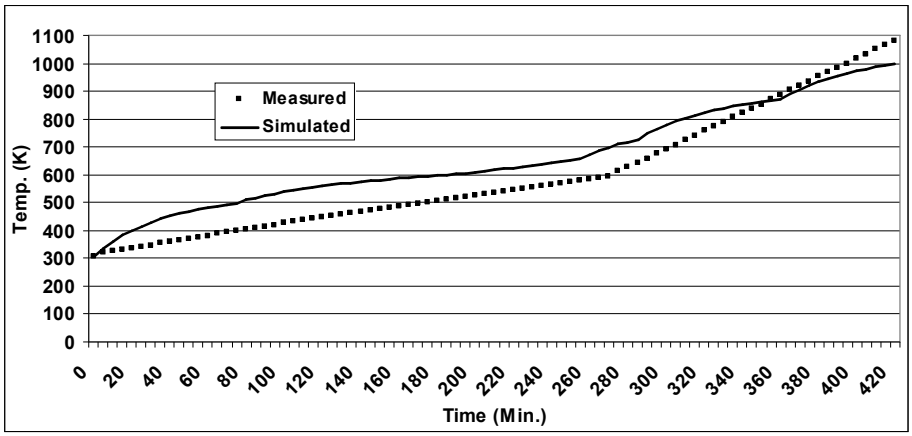

Figure 18: Comparison of predicted & measured ware temperatures, Kiln#4

Simulated temperature is a measure of average ware temperature and moves on both sides of the recorded Chamber Top temperature. The root mean square (rms) deviation is 17.14 %, which indicates a reasonable agreement.

6.2 Energy distribution in the kiln#4:

The pie-chart given in figure 19 indicates the predicted distribution of heat energy to various kiln components. The efficiency of the furnace is 7.34%. Energy transfer to the inner and outer walls is 35.55% and 1.94% respectively. This is due to the rat-trap construction of the inner wall. A very large amount of heat (55.1%) is being lost to the atmosphere with the exhaust gases.

6.3 Inferences from the experiment and simulation:

From the above we can infer that due the rat-trap construction for the inner wall, the heat absorbed by inner and outer wall has reduced to ~ 38%. The exhaust gas is taking away most of the heat (55.1%) and needs to be minimized by reducing the gas flow to the bare minimum to achieve complete combustion of the fuel.

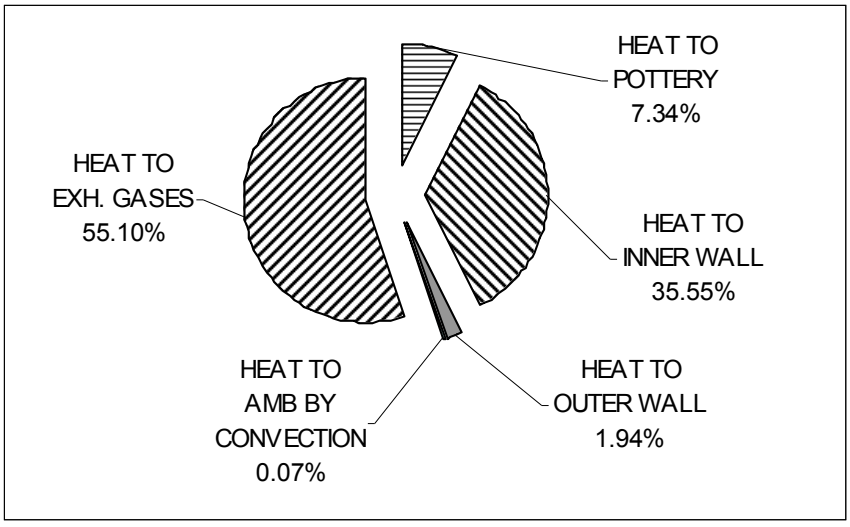

Figure 19: Distribution of heat to kiln components in kiln#4.

7.0 Conclusions:

1. The 1-D simulation model is successful in predicting the firing cycle of batch type ceramic kilns, of down draft as well as updraft type. The predictions are agreeing fairly in trend and values with the measurements.
2. The model is much simpler in estimating the gross temperatures than a 2 or 3 dimensional CFD analysis. The program does not need a high end PC.
3. The heat distribution pattern of Kiln#1&3 indicated that we need to reduce heat flow to the wall, by reducing thermal mass of the kiln, and to reduce the heat flowing out with flue gases, by reducing the gas flow through the kiln.
4. The energy distribution in Kiln#1 experiment was used successfully to design and build a laboratory scale kiln#2 of low thermal mass. The two experiments performed on Kiln#2 have again validated the simulation model. The heat distribution shows reduced heat flows to the inner wall and which improves the thermal efficiency.
5. Kiln#4 energy distribution shows that the change in inner wall construction has had the desired effect of reducing the thermal mass. The heat flow to the wall has reduced.
6. The overall performance of the model is good and it can be used to predict modified firing conditions to optimize the thermal efficiency of the system.

8.0 Acknowledgement:

The authors would like to thank Mr. Harkishan and MGIRI project personnel for their active cooperation in allowing us to collect the data (kiln#1 and kiln#4 respectively) at their premises, at New Delhi, and Wardha respectively.

9.0 References:

[1] K. N. Maiti, A. K. Gupta, Energy Conservation in Traditional Down Draft Kilns, Central Glass and Ceramic Research Institute, G.T. Road, Khurja 203131, 1993.

[2] K. Gupta, Wood-Fired Rural Kilns from Primitive to 2001, Chapter 10, Central Glass and Ceramic Research Institute, G.T. Road, Khurja 203131, 2001.

[3] K. Gupta, S. K. Biswas, S. Chakrabarty, Some Aspects of Firing in Down Draft Low Thermal Mass Kiln, Central Glass and Ceramic Research Institute, G.T. Road, Khurja 203131.

[4] M. Elhayek, P. Lybaert, H. Meunier, Investigation of CFD Technique to Study Energy Efficiency and product Quality in Ceramic Firing Kilns, Thermal Engineering Center, USA, March 2000.

[5] J. P. Holman, Heat Transfer, 9th edition, Tata McGraw-hill Publication Company, New Delhi, 2004.

[6] R H Perry & D W Greene, Perry's Chemical Engineering Handbook, 7th edition, McGraw Hill International Edition, New York, 1998.

APPENDIX - I

Kiln 1: System Description

The furnace studied was of the following specifications:

1. Inner dimensions	:	1.2 m x 1.2 m x 1.2 m
2. Inner lining	:	0.1125 m. Insulating brick
Density	:	1300 kg/m^3
Thermal conductivity	:	0.66 W/ ^{o}K. m
Specific heat	:	960 J/ kg ^{o}K
3. Outer insulation	:	0.1125 m ceramic blanket
Density	:	150 kg/m^3
Thermal conductivity	:	0.15 W/ ^{o}K. m
Specific heat	:	1070 J/ kg ^{o}K
4. Pottery-ware	:	Terracotta ware
Density	:	2000 kg/m^3
Thermal conductivity	:	1.32 W/ ^{o}K. m
Specific heat	:	840 J/ kg ^{o}K
5. Pottery-ware	:	110 kg of pre-fired terracotta ware.
6. Fuel used	:	Liquefied Petroleum gas (LPG), 70 kg was used.
7. Burner	:	Torch type, 8 no, maximum capacity of 2 lb/ hr each
8. Fuel Flow Rate	:	Measured by measuring weight of the 4 cylinders at a regular interval of 1 hour, using dial type weighing scale of +/- 0.5 kg least count.
9. Firing cycle	:	13 hour and 35 minutes, the ware were to be glazed to a temperature of 1075 ^{o}C or 1348 ^{o}K
10. Gas Composition	:	Measured using a portable gas analyzer for CO_2. Measured at every 30 minutes.
11. Chamber Temp.	:	Measured using R-type thermocouple and recorded every at every 30 minutes.

APPENDIX - II

Kiln 2: System Description

The furnace studied was of the following specifications:

1. Inner dimensions	:	0.3 m x 0.45 m x 0.6 m
2. Inner lining	:	0.225 m Ceramic Module
Density	:	128 kg/m^3
Thermal conductivity	:	0.11 W/ ^{o}K. m
Specific heat	:	1050 J/ kg ^{o}K
3. Outer insulation	:	0.1125 m Insulating Brick
Density	:	854 kg/m^3
Thermal conductivity	:	0.55 W/ ^{o}K. m
Specific heat	:	960 J/ kg ^{o}K
4. Pottery-ware	:	Terracotta ware
Density	:	2000 kg/m^3
Thermal conductivity	:	1.32 W/ ^{o}K. m
Specific heat	:	880 J/ kg ^{o}K
5. Pottery-ware	:	15.90 kg of pre-fired terracotta ware.
6. Fuel used	:	Liquefied Petroleum gas (LPG).
7. Burner	:	Torch type, 1 no, maximum capacity of 1 lb/ hr each
8. Fuel Flow Rate	:	Measured by a rotameter at a regular interval of 15 minute.
9. Firing cycle	:	5 to 7 hour, the biscuit ware were to be produced to a temperature of about 1000 ^{o}K.
10. Gas Composition	:	Measured using a portable gas analyzer for CO_2. Measured at every 15 minutes.
11. Chamber Temp.	:	Measured using R-type thermocouple and recorded every at every 15 minutes.

APPENDIX - III

Kiln 3: System Description

The furnace studied was of the following specifications:

1. Inner dimensions	:	dia. 1.83 m x ht. 1.21
2. Refractory/ insulation	:	0.5 m Red brick
Density	:	1997 kg/m^3
Thermal conductivity	:	1.25 W/ ^{o}K. m
Specific heat	:	880 J/ kg ^{o}K
4. Pottery-ware	:	Terracotta ware
Density	:	2000 kg/m^3
Thermal conductivity	:	1.32 W/ ^{o}K. m
Specific heat	:	880 J/ kg ^{o}K
5. Fuel used	:	Wood was used.
6. Fuel Flow Rate	:	Pre-measured quantities added and recorded every of 15 minute.
7. Firing cycle	:	5 to 7 hour, the biscuit ware were to be produced to a temperature of about 700 ^{o}K.
8. Chamber Temp.	:	Measured using thermocouple and recorded every 15 minutes.
9. Fire Box Temp.	:	Measured using thermocouple and recorded every 15 minutes.

APPENDIX - IV

Kiln 4: System Description

The furnace studied was of the following specifications:

1. Inner dimensions	:	dia. 1.5 m x ht. 1.65 m
2. Inner lining	:	0.2286 m Rat-trap bond construction with red brick
Density	:	1556 kg/m^3
Thermal conductivity	:	0.82361 W/ ^{o}K. m
Specific heat	:	880 J/ kg ^{o}K
3. Outer insulation	:	0.152 m Red brick
Density	:	2000 kg/m^3
Thermal conductivity	:	1.32 W/ ^{o}K. m
Specific heat	:	880 J/ kg ^{o}K
4. Pottery-ware	:	Terracotta ware
Density	:	2000 kg/m^3
Thermal conductivity	:	1.32 W/ ^{o}K. m
Specific heat	:	880 J/ kg ^{o}K
5. Fuel used	:	Wood was used.
6. Fuel Flow Rate	:	Pre-measured quantities added and recorded every of 15 minute.
7. Firing cycle	:	5 to 7 hour, the biscuit ware were to be produced to a temperature of about 700 ^{o}K.
8. Chamber Temp.	:	Measured using thermocouple and recorded every 15 minutes.
9. Fire Box Temp.	:	Measured using thermocouple and recorded every 15 minutes.

R_{wg}

List of figure captions

Figure 1: Sketch of 1-D analysis of the pottery kiln.

Figure 2: Radiation network between Pottery-ware, Gas and Kiln Wall

Figure 3: Simplified network between Pottery-ware, Gas and Wall

Figure 4: Mass & Energy Balance for the kiln.

Figure 5: Heat transfer in ware and wall domains

Figure 6: Schematic of a downdraft kiln#1

Figure 7: Comparison of predicted & measured chamber temperatures, Kiln#1

Figure 8: Distribution of heat to kiln components in kiln#1.

Figure 9: Schematic of a downdraft kiln#2

Figure 10: Comparison of predicted & measured chamber temperatures Kiln#2, Exp#1

Figure 11: Comparison of predicted & measured chamber temperatures Kiln#2, Exp#2

Figure 12: Distribution of heat to kiln components in Kiln#2, Exp#1

Figure 13: Distribution of heat to kiln components in Kiln#2, Exp# 2.

Figure 14: Schematic of a updraft kiln#3

Figure 15: Comparison of predicted & measured ware temperatures, Kiln#3

Figure 16: Distribution of heat to kiln components in kiln#3.

Figure 17: Rat-trap bond construction of the wall in kiln# 4

Figure 18: Comparison of predicted & measured ware temperatures, Kiln#4

Figure 19: Distribution of heat to kiln components in kiln#4.

List of Table captions

Table 1: Kiln#1 experiment: Instruments used for measurements

Table 2: Kiln#2 experiments: Instruments used for measurements

Table 3: Kiln#3 experiment: Instruments used for measurements